GA–A24244

IMPLOSION OF INDIRECTLY DRIVEN REENTRANT CONE SHELL TARGET

by
R.B. STEPHENS

AUGUST 2003

DISCLAIMER

GA–A24244

IMPLOSION OF INDIRECTLY DRIVEN REENTRANT CONE SHELL TARGET

by
R.B. STEPHENS

This is a preprint of a paper to be submitted for publication in *Phys. Plasmas.*

Work supported in part by
the U.S. Department of Energy under
Grant No. DE-FG03-00ER54606

GENERAL ATOMICS PROJECT 30078
AUGUST 2003

ABSTRACT

We have examined the implosion of an indirectly driven reentrant-cone shell target to clarify the issues attendant on compressing fuel for a fast ignition target. The target design is roughly hydrodynamic equivalent to a NIF cryo-ignition target, but scaled down to be driven by Omega. A sequence of backlit x-radiographs recorded each implosion. The collapse was also modeled with LASNEX, generating simulated radiographs. We compare experimental and simulated diameter, density and symmetry as functions of time near stagnation. The simulations were generally in good agreement with the experiments with respect to the shell, but did not show the opacity due to ablation of gold off the cone; non-thermal gold M-line radiation from the hohlraum wall penetrates the shell and drives this ablation causing some Au to mix into the low density center of the core and into the region between the core and cone. This might be a problem in a cryo-ignition target.

I. INTRODUCTION

The Fast Ignition (FI) Inertial Fusion Energy (IFE) concept is recognized as having the potential to improve the attractiveness of IFE reactors. FI ignites the dense core of separately compressed fuel pellets with a very intense laser pulse[1], achieving much higher gain than is possible with the baseline central hot spot approach[2]. Realization of this concept is somewhat complicated because the target core (~200 g/cc) is hidden under a plasma corona that is opaque for densities higher than ~0.01g/cc. A FI IFE target therefore must allow the possibility of efficiently converting the photons to a beam of charged particles that deposit their energy in a localized volume of the assembled core. In the initial conception, a laser pre-pulse was used to clear a path deep into the plasma and allow the ignition pulse to penetrate close to the core[3], where it could create a spray of ~MeV electrons. Experiments have shown efficient conversion to electrons[4], and tunnel digging[5], but it seems difficult to extend the digging sufficiently to get close to a very dense core. An alternative to ponderomotive tunneling is the use of a reentrant cone to exclude the plasma blowoff from one sector of the target; this allows the ignition laser a clear, close approach to the assembled core, and a controlled surface at which to create the electrons[6].

Targets of this form are extremely anisotropic. It is a question whether one could assemble a usable core from such a geometry; or even whether existing hydro models, which accurately describe the implosion of nearly symmetric targets, could accurately predict the implosion of a reentrant-cone-in-shell target. The presence of the reentrant cone near the core could cause turbulence, preventing a useful assembly of fuel, or cause contamination, preventing the assembled fuel from burning.

We set out to examine those questions; the purpose of this paper is to compare the experimental and modeled behavior of an indirect drive, reentrant-cone-in-shell target. The results of our experiment show that the target hydro is well modeled by standard codes, and the fuel is assembled in a reasonably compact form close to the density and form predicted by the simulation. However, some of the indirect drive spectrum (that from the non-thermal m-line emissions from the gold hohlraum) penetrates the shell and generates vapor from the surface of the gold cone. Turbulent mixing at the CH/Au interface apparently allows the gold vapor to mix into the low density center of the assembling target. It seems likely that most of this Au-laced gas is pushed back out of the shell toward the cone as the collapse continues. Future target designs should incorporate

cone designs that minimize the generation of high-Z contaminant, or should use direct drive.

II. EXPERIMENT

A cross-section of the target design is shown in Fig. 1b. It was scaled from the 1.8 MJ NIF ignition target in Fig. 1(a) to be driven with 14 kJ in a scale 1 hohlraum on Omega.

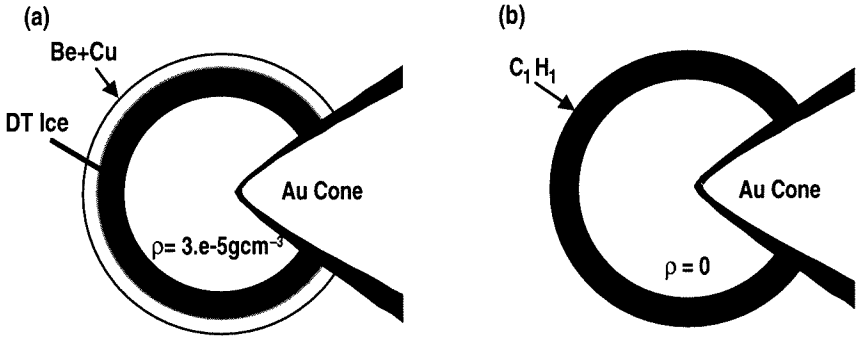

Fig. 1. (a) A NIF scale cryogenic ignition target consisting of a 2 mm o.d. Be shell surrounding a DT ice layer, into which a hyperboloidal cone is inserted. (b) Cross section of shell in (a) scaled down for OMEGA experiments.

The shell is 510 μm o.d. with a 57 μm thick plasma polymer wall. The cone is ~30 μm thick Au with a hyperboloidal tip (foci separation 40 μm) and a 35 deg. half angle [ftnt; hyperboloidal shape was chosen for modeling convenience]; the tip is 20 μm from the intersection of the asymptotes, and that is 12 μm from the center of the shell. The cone was attached to the shell with UV curing glue. This assembly was mounted in a hohlraum that had backlighter windows orthogonal to the hohlraum and cone axes (Fig. 2). The gold cone

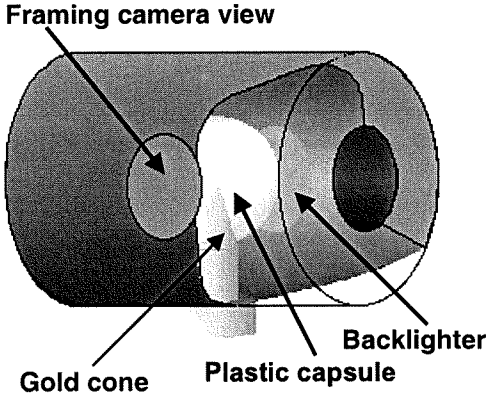

Fig. 2. Schematic of reentrant cone-in-shell target mounted in an Omega scale 1 hohlraum. The 7 μm thick Cu backlighter foil is mounted on the hohlraum wall behind the shell; the x-ray framing camera looks at the target from the other side through a 50 μm thick CH window with 0.15 μm thick Ta coating on the inside.

was stepped to minimize interference with adjacent high angle laser beams, and to avoid creating hot spots on the cone surface close to the shell; either effect would have distorted

the drive. Forty drive beams were oriented as for a standard indirect drive shot and driven using pulse shape 26.

We used Fe (6.7 keV for He-like Fe) illuminated by 20 beams to backlight the target for an x-ray framing camera that took images through a 10 μm pinhole at ~70 ps intervals. The fixed structure in the images was eliminated by reference to a flat-field image (e.g. camera was illuminated with an open aperture instead of a pinhole)[11]. One pixel wide streaks in the image, from pixel defects, were replaced with the adjacent row of pixels. Then the images were smoothed using a 5 μm boxcar average.

This sequence of pictures clearly shows the evolution of the shell and cone [Fig. 3(a) – only every other image is shown]. An equivalent (including pixelation, time-smearing, and smoothing) set of pictures was generated from a LASNEX[12] simulation of the implosion [Fig. 3(b)]. For both set of images, profiles were taken from a 15 μm wide, 300 μm long

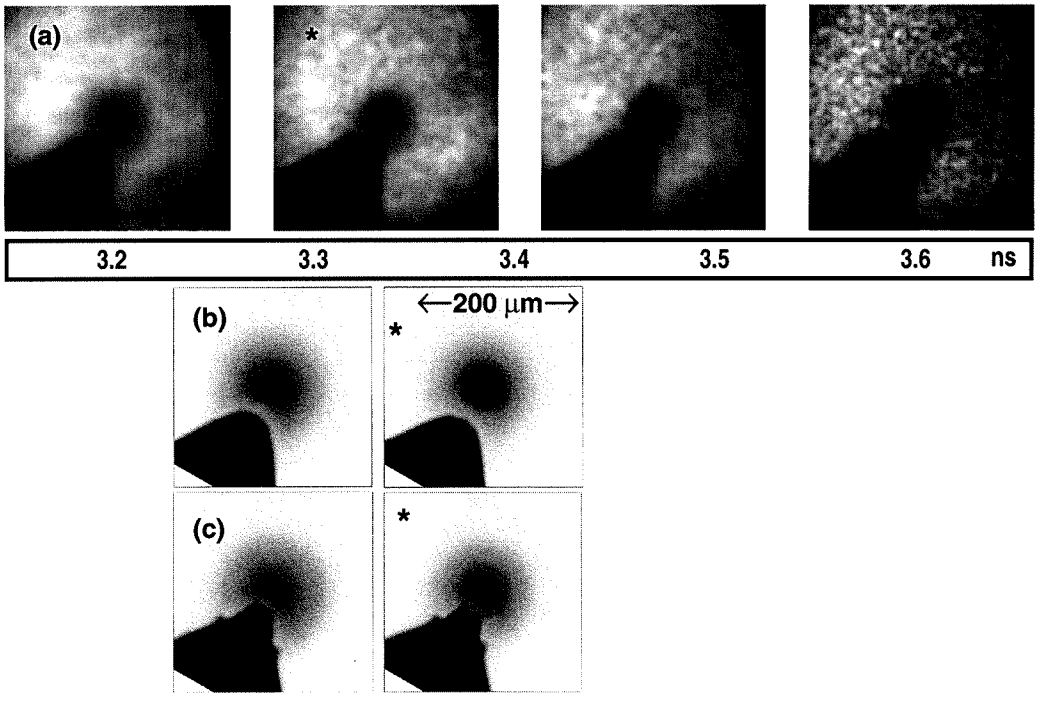

Fig. 3. X-radiograph sequence of shell collapse (a) experimental results, (b) simulated collapse sequence at 140 ps intervals. The stagnation points (the *ed images — 3.33 and 3.4 ns for expt and simulation, respectively) are set under one another. (c) Shows the experimental image at stagnation using a log gray scale, and with a white divider between the black and the gray, so one can see that the experimental cone shadow (black) is very similar to the model, but has been extended by nearly opaque (dark gray) blowoff from the cone.

strip perpendicular to the cone axis. Backlighter brightness along that path was estimated by fitting a parabola to the intensity seen at each end of the strip. Experimental dark counts were estimated from counts between illuminated sections.

Using the brightness and background, we calculate the x-ray optical depth vs. position across the apparent center of each image for both the experimental and simulated images (Fig. 4), the full width half density size of the assembled target as a function of time (Fig. 5).

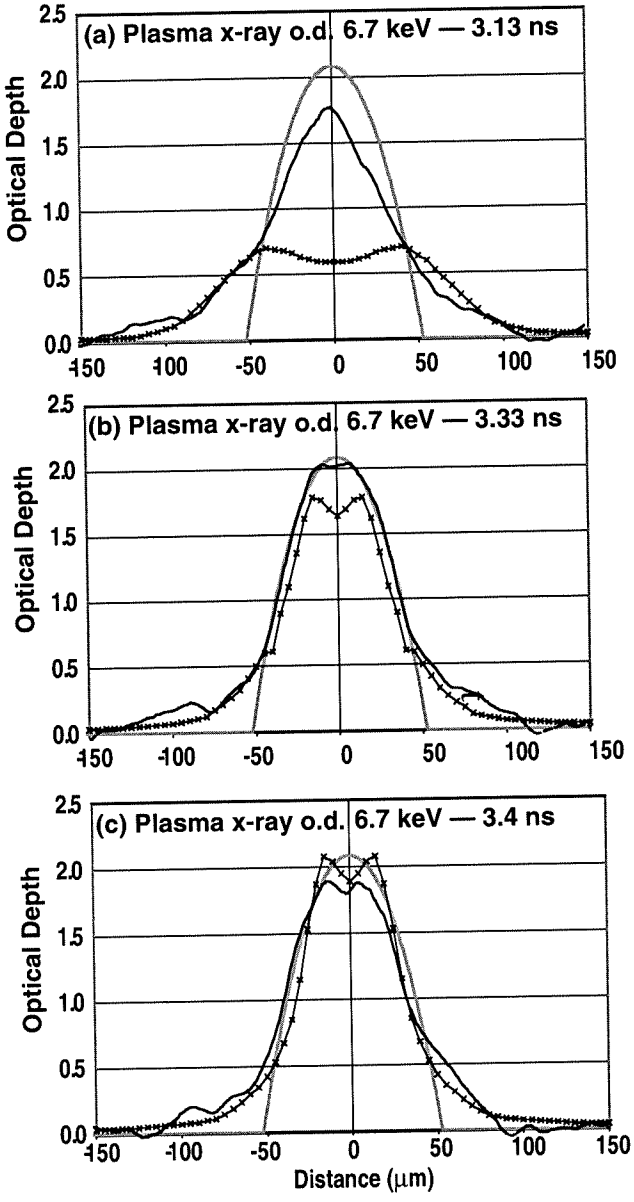

Fig. 4. Comparison of the experimental and simulated profiles (a) before, (b) at and (c) after stagnation. The profile of a uniformly dense sphere is shown in each graph as reference. The profiles were taken along a line through the center of the mass, perpendicular to the cone axis.

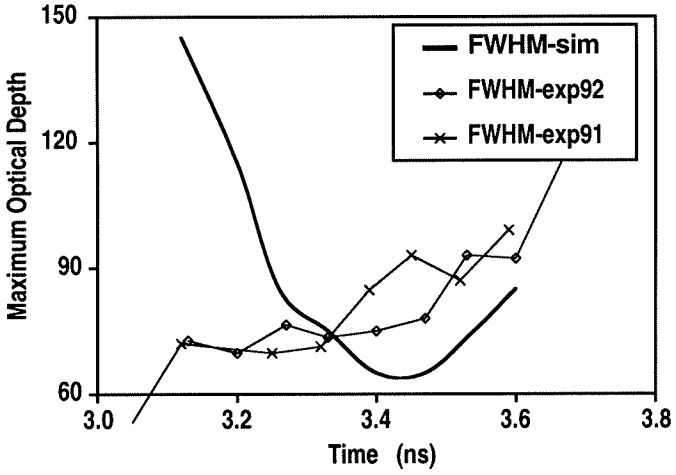

Fig. 5. Full width at half absorption of profiles as a function of time for simulation and experiment.

II. DISCUSSION

The collapsing shell's stagnation time (3.3 ns), f^{whm} size (70 μm), and maximum x-ray optical depth (2), agree with the model (3.4 ns, 65 μm, and 2, respectively), the gross structure of the collapsing shell (horseshoe crab-like) looks very much as predicted, and we assembled about the expected fraction of the mass (m/m_o = 28±4% — calculated from the lineouts ignoring the cone and assuming spherical symmetry to the collapsing mass). But there are significant differences: the experimental profiles lack the hollow center and show an increase in maximum optical depth that ought to be observable, especially at early times (Fig. 4) and a decrease in f^{whm} as the shell collapses (Fig. 5). More noticeably, the apparent cone shadow extends much closer to the shell than predicted. We believe these effects are connected. Most of that shadow is merely dense vapor [(Fig. 3(c)]. The very opaque region (solid gold) is marked off by the white line in Fig. 3(c); the rest of the shadow transmits a few to 10% of the backlight (~1 g/cc of Au). The model x-ray drive included the non-thermal M-line radiation from the gold hohlraum. In the simulations these high energy x-rays penetrate the capsule and heat the tip of the cone, causing ablated gold plasma to extend nearly out to the center of the collapsing shell as seen in the experiment (Fig. 6). Later, as the capsule collapses, plastic plasma blown off the

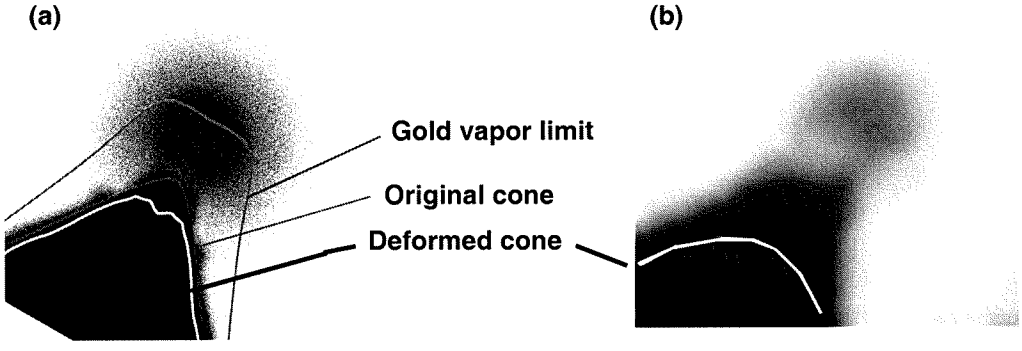

Fig. 6. (a) Simulated and (b) experimental x-radiograph at stagnation with lines showing the original and deformed cone profile, and extent of gold vapor expansion. The simulated image was done without accounting for the gold vapor. The experimental image uses a logarithmic gray scale to show the transmission through the gold vapor.

inside of the shell by shock waves impinges on the gold plasma with a pressure gradient that tries to push the gold plasma back toward the cone tip, but the Au vapor is dense enough that the boundary is unstable, so some mixing is expected. This instability, however, is *not* captured by our simulations, mostly because the interface was not "seeded" with any perturbations. Therefore, in the simulations the gold plasma *is* pushed back with the result that there is no significant opacity in the space between the core and

the cone. In reality we expect the interface to be quite perturbed with the result that the gold plasma would not be pushed back toward the cone but would instead be mixed with the plastic plasma in the interface region resulting in the opacity seen in the experiment. This effect (which could be quite detrimental to full scale FI) should not occur if the capsule is directly driven. An experimental test of this hypothesis is currently being undertaken.

Assuming that the difference between experiment and simulation in Fig. 4(a) is caused by Au vapor in the low density core, one concludes that the core contains ~0.4 g/cc of Au vapor. [ftnt: using s_{Au} = 332 cm^2/gm; the simulation indicates that the core is heated to ~400 eV, which strongly bleaches the C absorption there, but has little effect on the Au.]

The strong central absorption decreases in successive pictures and becomes, at stagnation that of a uniformly dense solid [(Fig. 4(b)]. It is highly unlikely that the gold could mix throughout the dense shell in such a short time. Much more likely is that much of the Au was ejected from the collapsing shell along with the rest of the low density core. In the simulation that gas is moving toward the tip of the cone at ~0.3 μm/ps.

We estimate that the Au amounted to ~0.4 wt% of the collapsed mass. That would be fatal in the scaled up cryo-ignition target; 0.1wt% is sufficient to double the required ignition energy. It seems difficult to eliminate the non-thermal x-ray source since alternative hohlraum materials and mixtures ("cocktail hohlraums") all have fluorescent lines in the range1-4 keV. At ignition scale, the shielding against those lines is much better; a NIF scale shell would have a doped ablator wall (~100 μm of Be:Cu0.0[2]) that is ~5 times the 2 keV absorption length. We have not attempted to calculate the Au ablation and mixing at ignition scale.

III. CONCLUSION

The presence of the reentrant cone causes gross changes in the collapse that are reasonably well described by LASNEX modeling; this suggests that the hydro-equivalent, NIF scale, cryo-ignition target would implode to a useful ρR. However, non-thermal emissions from the gold hohlraum vaporized gold off the outside of the reentrant cone, and this vapor apparently mixed into the low density core of the assembled fuel. This contamination is potentially serious for indirect drive; adding 0.1 wt% Au doubles the required ignition energy. Alternatively, using direct-drive geometry[9, 10], would avoid the problem entirely.

ACKNOWLEDGMENTS

We gratefully acknowledge the fabrication by J. Smith and assembly by S. Grant of the complex targets used for these experiments. We are indebted to the Omega team for operational support. This work was performed under the auspices of the U.S. Department of Energy under Contract DE-FG03-00SF2229 with the University of California, Lawrence Livermore National Laboratory under Contract W-7405-ENG-48, and with the additional corporate support of General Atomics.

REFERENCES

[1] M. Tabak, *et al.*, *Phys. Plasmas* **1**, 1626-1634 (1994).

[2] M. Rosen, *Phys. Plasmas* **6**, 1690-1699 (1999).

[3] A. Pukhov and J. Meyer-ter-Vehn, *Phys. Rev. Lett.* **79**, 2686 (1997).

[4] M.H. Key, *et al.*, *Phys. Plasmas* **5**, 1966-1972 (1998).

[5] A.J. Mackinnon, *et al.*, *Phys. Plasmas* **6**, 2185-2190 (1999).

[6] M. Tabak, E.M. Campbell, J.H. Hammer, W.L. Kruer, M.D. Perry, S.C. Wilks, and J.G. Woodworth, Lawrence Livermore National Laboratory Patent Disclosure, IL-8826B, 1997, Lawrence Livermore National Laboratory, Livermore CA.

[7] R. Kodama, *et al.*, *Plasma Phys. Control. Fusion* **41**, A419-A425 (1999).

[8] R. Kodama, *et al.*, *Phys. Plasmas* **8**, 2268-2274 (2001).

[9] R. Kodama, *et al.*, *Nature* **412**, 798-802 (2001).

[10] R. Kodama, *et al.*, *Nature* **418**, 933-934 (2002).

[11] O.L. Landen, *et al.*, *Rev. Sci. Instr.* **72**, 627-634 (2001).

[12] J. Harte, *et al.*, *1996 ICF Annual Report*, Lawrence Livermore National Laboratory, Livermore CA, UCRL-LR-105821-96, 150 (1997). Available online at http://www.llnl.gov/tid/lof/documents/pdf/233052.pdf.